Cyclic and post-cyclic geocell pullout behavior in cohesionless soil

Ali Namaei-kohal[1]

Alireza Ardakani[2]*

Mahmoud Hassanlourad[3]

[1]Department of Civil Engineering, Imam Khomeini International University, Qazvin, Iran, Email: namaeiali@yahoo.com, Phone number: +982833901160, Address: Qazvin, Iran, Imam Khomeini International University.

[2]Department of Civil Engineering, Imam Khomeini International University, Qazvin, Iran, Email: a.ardakani@eng.ikiu.ac.ir, Phone number: +982833901160, Address: Qazvin, Iran, Imam Khomeini International University.

[3]Department of Civil Engineering, Imam Khomeini International University, Qazvin, Iran, Email: hassanlou@eng.ikiu.ac.ir, Phone number: +982833901190, Address: Qazvin, Iran, Imam Khomeini International University.

Corresponding author: Email: a.ardakani@eng.ikiu.ac.ir, Phone number: +982833901160

Abstract

This research investigated the cyclic and post-cyclic pullout behavior of geocell in cohesionless soil using a series of 24 multi-stage pullout tests. To control the number of pullout tests, only the effect of the effects of cyclic loading amplitude, number of cycles and load frequency are evaluated and other parameters are assumed to be constant. The results indicated that the ultimate post-cyclic pullout load was less than the monotonic pullout load. This was the result of a reciprocating motion from loading caused by the interlock between the geocell infill soil and the surrounding material, which weakened and broke during the cyclic phase. It was found that, as the grain size of the soil increased, the interlocking strength increased and consequently the ultimate post cyclic pullout load increased. The soil particle size had a significant effect on the cumulative displacement during the cyclic phase. Furthermore, the increases in the loading amplitude and the number of cycles decreased the interlocking resistance of the infill soil with the surrounding material, which decreased the ultimate post-cyclic pullout load. The effect of the loading frequency likely depended on the geocell infill soil density.

Keywords: Cyclic; Post-cyclic; Geocell; Pullout testing; Soil-geosynthetic interaction

1. Introduction

Urban structures are increasingly likely to be constructed on weak soil. There are so many different geotechnical methods to improve these soils. These methods contain using pile and micro-pile systems, chemical soil improvements, dynamic compaction and etc [1-5]. Geosynthetic reinforcement is a common soil-improvement technique that is designed to stabilize weak soil. Geocells are three-dimensional (3D) cellular geosynthetics that have been used to improve the performance of pavement and railway beds, to avert landslides, and under pipelines, embankments and retaining walls [6-13].

Most of the studies that have been conducted on the geocell reinforcement performance were based on the monotonic loadings, however, different types of dynamic loadings are being applied to the reinforced structures over their service life. Therefore, the response of geocell reinforcement to dynamic loads should be evaluated. Tafreshi and Dawson [14] compared the behavior of geocell reinforced foundations under monotonic and cyclic loading. They showed the efficiency of geocell reinforcement in reducing the foundation settlement. Moreover, the presence of geocells limited

plastic deformation under cyclic loading more than a similar geocell monotonic loading. Latha and Manju [15] assessed the seismic behavior of physically modeled geocell retaining walls. They found that the increase in seismic loading parameters showed more effect on the retaining wall behavior than the increase in geocell layer parameters. Biabani et al. [16] evaluated the performance of a physically modeled geocell reinforced sub-ballast under railway cyclic loading. They indicated that the lateral displacement of the sub-ballast was reduced by increasing geocell stiffness. Also, they conducted a series of numerical simulations to measure the induced stress in geocell cells showing the dependency of maximum mobilized stress on the geocell stiffness. Pokharel et al. [17] used three types of granular materials investigate the behavior of geocell reinforced bases under repeated loading. The results demonstrated that the presence of geocell decreased the plastic deformation and increased the elastic deformation under cyclic loading. Xinye et al. [18] also compared the behavior of geocell and geogrid reinforced retaining walls through a series of shaking table tests. They illustrated that the geocell reinforced retaining wall showed higher ductility and damping than the geogrid reinforced wall under seismic loading, although, the obtained dynamic resistances of these two reinforcements were the same. Venkateswarlu et al. [19] compared geocells and geogrids reinforced a machine foundation. The results showed that the presence of geocell led to a decrease in the resonant amplitude and peak particle velocity in comparison with unreinforced foundation. In this comparison, the natural frequency of the soil system was also increased by placing geocell. The aforementioned studies mostly discussed the effect of the geocell mattresses for reinforcing different geotechnical structures under different dynamic loadings. However, geocell reinforcing mechanisms under different types of loadings should be evaluated, as well. Also, Venkateswarlu et al. [20-21] and Venkateswarlu and Hegde [22-24] performed a series of numerical modeling and experimental tests to assess different aspects of geocell reinforced soil bed behavior under dynamic loadings. From the studies, they stated that reinforcing the soil bed with geocell was found to be a worthwhile approach to control the vibration parameters. It was found that a significant reduction in ground vibration was observed in the presence of geosynthetics. Maximum reduction was observed in the case of geocell reinforced condition as compared to other cases. They observed that 98% improvement in the stiffness of the foundation bed was occurred in the presence of geocells. Furthermore, the dynamic response obtained

from the field study was compared with the mass spring dashpot analogy. The dynamic response predicted from the analytical study has shown reasonable agreement with the test results.

Zhao et al. [25] identified passive resistance, shear resistance, and vertical load distribution are the main components of a geocell reinforcing mechanism. The first two components control the interfacial behavior of a geocell and are significant in the design process of a geocell mattress. Also, Tavakoli and Motarjemi [26] investigated the shear behavior of geocell-reinforced sandy and gravely soils using large-scale direct shear tests. The results led them to recommend the use of geocells in cases with low-normal stress and large main particle sizes. They increased the soil aggregate size and observed a significant increase in the geocell interfacial strength. They suggested the use of geocells with a cell diameter to the medium-grain-size ratio of 4 to produce the best interfacial performance. On the other hand, to assess the passive resistance component, pullout tests should be performed (Isik and Gurbuz [27]). Moreover, the total capacity of the geocell reinforced should be evaluated to use in the design process, as in practical projects (such as retaining walls, slopes, embankments, etc.) the geocell mattresses can be subjected to pullout loading. Khedkar and Mandal [28] investigated the pullout behavior of a cellular reinforcement. They showed that the pullout resistance increased with the increase in the cellular reinforcement height to a specific value. Then the pullout resistance decreased due to the higher interaction with transverse elements. They also suggested the interaction coefficient of the cellular reinforcement which was increased by increasing the reinforcement height. Han et al. [29] evaluated the interaction between geocell reinforcement and gravely soil by pullout test. They found that the pullout capacity is composed of two factors: the shear resistance along the shear bands developed at the top and bottom interfaces between the geocell and the adjacent backfill and the anchorage resistance induced by passive pressure inside the aperture of the geocell, which increases and becomes more dominant in the total pull-out resistance with an increase in the height of geocell. Biabani et al. [16] also evaluated the pullout resistance and the interfacial behavior of geocells. The behavior of the geocell reinforcement depended on the loading mechanism, friction coefficient, and geocell modulus. The geocells mobilized at higher passive resistance values in the pullout test than in the large-scale direct shear test and this was related to the different geocell

reinforcing mechanisms for mobilization in each of these tests. Isik and Gurbuz [24] redesigned the conventional pullout test apparatus to assess the pullout resistance of a geocell mattress in sandy soil under monotonic loading. This large-scale test on 3D geosynthetics showed that the pullout resistance increased with an increase in the geocell length, width, height, and stiffness, although the total pullout resistance was limited by the strength of the longitudinal and transverse strip junctions. A large amount of strain was induced near the geocell front in this study but gradually decreased toward the end of the geocell. Furthermore, they evaluated an analytical method to calculate each geocell reinforcing mechanism for geocells with a square pattern. Also, Fakharian and Pilban [30] assessed the pullout resistance of diagonally enhanced and conventional geocells in sandy soil. Both the stiffness and ultimate resistance of the diagonally enhanced geocells improved significantly compared to the conventional geocells. They conducted three tests on a physical model of a shallow footing reinforced with geocells. The results showed an improvement in bearing capacity and the load-settlement response of the footings supported on the new geocells compared to the conventional geocells.

It can be seen that the previous research on geocell mattress pullout resistance and reinforcing mechanism was done under monotonic loadings. On the other hand, a geosynthetic reinforced structure may be subjected to the both pullout load and earthquake load. It is known that a static pullout load applies on the geosynthetic through the backfill meanwhile if the backfill subjected to a dynamic loading like earthquake or traffic loading, this dynamical loading can be passed to the geosynthetics through interaction mechanisms and pullout capacity will be determinative in design process. There were so many literature evaluated the behavior of a geosynthetic reinforced structure under seismic loads [31-33]. Therefore, it is essential to investigate the pullout resistance and reinforcing mechanisms of geocell mattresses under cyclic loading and consider the cyclic conditions during the design process if necessary. In the current study, 24 three steps pullout tests were carried out to evaluate the cyclic and post-cyclic geocell pullout resistance and interfacial properties of three types of cohesionless soil. Furthermore, the effect of cyclic loading amplitude, number of cycles, load frequency, and cumulative displacement has been examined on the ultimate pullout load and pullout load-displacement behavior of geocell in detail.

2. Experimental program

Three types of granular soils were used to evaluate the cyclic and post-cyclic pullout behavior of the geocells. Their properties are given in Table 1 and Fig. 1 shows the soil grain-size distribution. These materials were classified as SP and GP according to the Unified Soil Classification System. The maximum and minimum unit weights of the soil types were measured using a vibration table test for the poorly graded samples according to ASTM D4253 [34] and ASTM D4254 [35], respectively. Moreover, the geocell mattresses used in this study, were manufactured of polyethylene strips covered with multiple rhomboidal indentations on the both sides. Each strip was ultrasonically welded at fixed intervals to produce cellular honeycombs. The parameters are given in Table 2. The strength properties of the geocell was calculated according to ASTM D4595 [36]. A common pullout apparatus shown in Fig. 2 was used that was composed of a large box of 90 cm in length, 50 cm in width, and 50 cm in depth. Vertical pressure was applied through the use of an airbag which applied 75 kPa of maximum pressure. The pullout force was applied using a two and half-ton hydraulic jack with the ability to apply 75 mm of maximum displacement at up to 100 Hz. To avoid boundary effects, acrylic glasses were attached to the sides of the pullout apparatus box.

To perform the pullout test, the dry granular materials were held in 20-kg plastic bags. To reach 70% relative density for each soil, the amount of soil required to reach the relative density was measured according to the maximum and minimum unit weight tests. It was found that the prepared samples in each of these 20-kg bags should be placed in 4 cm, 3.5 cm and 3 cm thick layers for sand, gravel 1, and gravel 2, respectively, to reach 70% relative density. Hence, each soil sample was poured into the lower half of the pullout box and vibrated until the thickness of the layer reached the calculated value (4- cm for sand, 3.5- cm for gravel 1, and 3-cm for gravel 2). As the used soils were poorly graded, these soils compaction with hammer or any other method except from vibration wasn’t effective and the soils wouldn’t compact. The vibration method used in this for compaction. As this method can lead to the higher density than 70%, the density should be measured in each layer. To control the achieved relative density, a small steel cylindrical container was placed in different positions inside each soil layer after each layer compaction. The weight and the volume of this cylindrical container

were measured and accordingly the density of soil calculated. Same procedure was performed by Mahigir et al. [37].

Upon reaching the middle height of the pullout box, a geocell of 800 mm in length and 40 cm in width was placed on the soil (Fig. 3). To minimize sidewall friction, a minimum 75-mm space was maintained between the edge of the geocell and the edge of the box according to ASTM D6706 [38]. The geocell was attached to a two and half-ton hydraulic jack with the ability to apply 75 mm of maximum displacement at up to 100 Hz. A new clamp was designed to attach the 3D geosynthetic to the hydraulic jack. A plate of 2.5 mm in thickness was welded to a 12-mm pipe at the point at which the geocell was attached to the 10-mm clamp. Two vertical plates of 3 mm in thickness were placed on each side of the geocell wing to avert rupture at the connection during the pullout test. The front of the clamp was drilled and attached to the hydraulic jack (Fig. 4), then the geocell was attached to the jack.

To measure displacement at different parts of the geocell during the test, wires were attached to the centers of each geocell cell row. These wires, as shown in Fig. 3, go through metal rods to avoid any damage to the wires and also avoid any interaction. At the end of the box, there are holes. Rods were finished in there and the wires are attached to the LVDTs. These wires were passed through the back wall of the box connected to the LVDTs were attached to LVDTs at the back of the box. To reach a firm attachment between wires and the geocell walls, a 4 mm hole was created at the attachment place. Each wire was tied to a hook and the hook was attached to the geocell wall (Fig. 5). At last, each geocell cells were fixed at their placed by some bolts. After the geocell layer was prepared, each cell of the geocell was filled with the amount of soil required to attain the specified relative density. Then, the fixity bolts were removed to let geocell deform freely during the tests. Next, the upper half of the pullout box was filled with granular materials in the same manner as the lower half. The airbag was placed on top of the granular material to apply either 20 or 60 kPa of vertical

pressure. This airbag was attached to an air compressor and the value of air pressure was controlled with compressor gauge during the test.

The box was secured and closed with bolts before the application of the vertical pressure. Then, the multi-stage and monotonic pullout tests were conducted.

The monotonic tests were conducted under 1 mm/min rate of displacement until a rupture occurred at the geocell or the geocell reached 75 mm of frontal displacement. The multi-stage pullout tests were performed in three stages. Initially, the pullout test was conducted at a constant rate of 1 mm/min until the force reached a specific ultimate monotonic pullout load (P_m) under 20 and 60 kPa of vertical pressure. Moraci and Cardile [39] showed that the cyclic stage of 2D geosynthetics initiated at 0.2 to 0.4 P_m; thus, 0.4 P_m was chosen to initiate the cyclic stage and evaluate the cyclic and post-cyclic behavior of the geocell as well as the 2D geosynthetic. In the cyclic stage, a control sinusoidal-force pullout load was applied at 0.1 and 1 Hz at amplitudes (A) of 0.2, 0.3, and 0.4 P_m. The cyclic load was applied for 10 and 30 cycles (N) and the test continued under a 1 mm/min rate of displacement to evaluate the post-cyclic behavior of the geocell. Testing continued until a rupture occurred at the geocell or the geocell reached 75 mm of frontal displacement.

3. Results and discussion

3.1. Monotonic and multi-stage pullout behavior

Figs. 6 and 7 show the monotonic and multi-stage pullout behavior of geocells in sandy and gravely soils under 20 and 60 kPa of vertical pressure, respectively. It can be seen that the geocell reached a lower ultimate pullout load in all multi-stage tests than the monotonic one in each soil type under both 20 and 60 kPa of vertical pressure. This can be related to the reciprocating motion during cyclic loading which weakened and broke some of the interlockings of geocell infill and geocell walls. Consequently, this effect led to reach a lower ultimate pullout load in the multi-stage tests than in the monotonic tests. On the other hand, Fig. 6(a) shows that the pullout load decreased at a frontal displacement of 63 mm, indicating that most of the interaction between the infill material and

surrounding sandy soil had broken. The pullout load continued at 8 kN and the passive resistance in each geocell pocket due to the adjacent cell mobilized at up to 75 mm of frontal displacement.

The obtained results demonstrated in Figs. 6 and 7 also indicate that the monotonic ultimate pullout load decreased 15% in sandy soil under 20 kPa of vertical pressure in the multi-stage test. The decreases were 11% and 9% for gravel 1 and gravel 2 under the same vertical pressure, respectively. It can be inferred that the shear resistance between the geocell and surrounding soil increased as the soil particle sizes increased and the interlock was harder to break in coarser soil as the cyclic loading characteristics were kept constant. The increase in vertical pressure led to a decrease in the difference between monotonic and multi-stage ultimate pullout test results and the ultimate pullout loads decreased 13%, 10%, and 5% for sand, gravel 1, and gravel 2 under 60 kPa of vertical pressure, respectively. This shows that, for the same soil particle size, the increase in vertical pressure stiffened the geocell-soil interaction and decreases the difference between ultimate monotonic and multi-stage pullout load. Moreover, Fig. 7(a) shows that the monotonic test did not reach a steady-state because not all of the geocell pullout load capacity had mobilized at 75 mm. This is in contrast with the multi-stage test graph. The cyclic phase for sandy soil under 60 kPa decreased the geocell membrane mechanism and reached a steady-state in the post-cyclic phase. However, not all of the reinforcing mechanisms mobilized in the monotonic test and greater frontal displacement were needed to reach the total pullout resistance of the geocell.

To investigate the behavior of geocell along the 80 cm length, the activated length was measured during monotonic and multistage tests. When LVDTs attached to the middle of each geocell row started to record displacement, that length of geocell was considered as activation length. The obtained activated length versus pullout load is demonstrated in Fig. 8. It can be seen that all the geocell length contributing to pullout resistance was activated in all tests except for the monotonic test in sandy soil under 60 kPa vertical pressure where only up to the middle of third row was activated. It shows that a higher pullout load was needed to activate all of the geocell lengths in this condition. Furthermore, increases in either the vertical pressure or soil particle size caused the development of pullout load in the first cellular row. This behavior was similar in the other geocell cellular rows, but the rate of the pullout load needed to activate the second and third rows decreased. This result may

indicate that the first geocell row mostly carried the load when either the vertical pressure or soil particle sizes were increased or the geocell needed a higher pullout load to deform. Also, the geocell length activated in lower pullout load during multi-stage tests in comparison with monotonic test results. This is related to the interaction loss after applying cyclic loading. Therefore, the geocell displace more during multi-stage tests and each of the geocell cell rows activated in lower pullout load. However, it can be seen in Fig. 8(a) that the first row of the geocell in multistage and monotonic tests in sandy soil under 20 kPa vertical pressure has activated in the same pullout load because the cyclic phase initiated at 20 mm frontal displacement according to Fig. 6(a).

3.2. Effect of load amplitude and cumulative displacement

The multi-stage test results for amplitudes of 0.2, 0.3, and 0.4 P_m in gravel 2 are shown in Figs. 9 and 10 under 20 and 60 kPa of vertical pressure, respectively. It can be seen that the increase in cyclic load amplitude from 0.2 to 0.3 and 0.4 P_m caused the ultimate post-cyclic pullout load to decrease by 2% and 4% under 20 kPa of vertical pressure, respectively. Figs. 9 and 10 indicate that this reductive effect decreased as the vertical pressure increased and the increase in load amplitude from 0.2 to 0.3 and 0.4 P_m led to a decrease in the ultimate post-cyclic pullout loads of 1% and 3%, respectively. The effect of amplitude indicates that the weakening and breaking of the geocell-soil interlock developed when the cyclic load was applied at a higher amplitude. This effect decreased at a higher vertical pressure as the interlocking between the geocell infill soil and the surrounding soil was harder to break. Correspondingly, the same behavior was seen in sandy soil and gravel1. In order to assess the load amplitude effect in sand and gravel1, the ratio of ultimate multi-stage pullout load to ultimate monotonic pullout load for each test was calculated using Eq. (1) and is given in Fig. 11. It can be seen that the geocell pullout load in sandy soil at 0.4 P_m and 20 kPa of vertical pressure decreased to about 15% of the ultimate monotonic pullout load and the pullout load decreased to 12% and 9% in gravel 1 and gravel 2, respectively, under the same loading conditions. The obtained results show that the reductive effect of an increase in the cyclic load amplitude increased as the soil particle size became finer because of the decrease in the soil-to-infill soil interaction.

$$R = \frac{ultimate\ multi\ stage\ pullout\ load}{ultimate\ monotonic\ pullout\ load} \quad (1)$$

Furthermore, the soil particle size and load amplitude affected the cumulative displacement during the cyclic phase. Fig. 12 shows that the cumulative displacement during the cyclic phase decreased as the soil particle size and vertical pressure increased. The cumulative displacement in sandy soil under 20 kPa of vertical pressure and 0.2 P_m of load amplitude was 4.7 mm. This value became 4.2 mm at 60 kPa of vertical pressure and 0.2 P_m of load amplitude. When the loading characteristics were held constant, the cumulative displacement decreased from 4.7 mm in sandy soil to 3.3 and 3.1 mm in gravel 1 and gravel 2, respectively. This indicates that, as the interaction between the geocell infill soil and surrounding soil stiffened, the cumulative displacement decreased. A stiffer interaction was reached with an increase in the vertical pressure and soil particle size. By contrast, the increase in load amplitude from 0.2 to 0.4 P_m caused some of the interlock between the infill materials and surrounding soil to break and the geocell to displace easily during the cyclic phase.

3.3. Effect of frequency and number of cycles

The multi-stage load-displacement behavior of the geocell at 0.1 and 1 Hz and 0.4 P_m of load amplitude under 20 kPa of vertical pressure in gravel 1 are shown in Fig. 13. Also, Table 3 shows the cumulative displacement and R values for tests at 1 Hz and 0.2, 0.3, and 0.4 P_m of load amplitude under 20 kPa of vertical pressure in gravel 1. It can be seen that the increase in loading frequency to 1 Hz led to increase the ultimate pullout load in post cyclic phase where there wasn't any significant differences between the ultimate pullout load obtained from multi-stage and monotonic tests. However, the ultimate pullout of the multi-stage test at 0.1 Hz was 10% lower than the ultimate pullout of the monotonic test. Moreover, an increase in load frequency considerably decreased the cumulative displacement during the cyclic phase and the ultimate post-cyclic pullout load at different loading amplitudes.

Similar results were reported by Zuo et al. [40] for the effect of frequency on planar geosynthetics. However, Moraci and Cardile [39] reported that frequency had no significant effect on the pullout behavior and Mahigir et al. [37] reported a reductive influence of frequency on the pullout behavior of

geogrid. These different results indicate that the effect of the loading frequency on the pullout behavior of geosynthetics depended on the properties of the geosynthetic, soil, and frequency content. In this evaluation, the enhancing effect of load frequency can be related to the increase of geocell infill soil density as the applied vibration can compact a poorly graded granular materials like gravel 1 and by increasing the load frequency caused to obtain a higher ultimate post cyclic pullout load.

Fig. 14 shows the multi-stage test results after 30 cycles at 0.4 P_m of load amplitude and 0.1 Hz under 20 kPa of vertical pressure. It is evident that the post-cyclic phase did not occur in sandy soil and the geocell reached 75 mm of frontal displacement during the cyclic phase. This behavior indicates that the interlock between the geocell infill soil and the surrounding soil was lost, causing a significant increase in displacement during cycles 1 to 4. The rest of the cycles were applied at 55 to 75 mm, where only passive resistance in each geocell cell contributed to the cyclic pullout load. The steady-state of the post-cyclic phase was reached for gravel 1 and gravel 2 because the increase in the number of cycles failed to break the gravel-to-infill soil interlock completely. The ultimate post-cyclic pullout loads in gravel 1 and gravel 2 were 14% and 12.5% lower than the ultimate monotonic pullout loads because of the loss of some of the interlock between the infill soil and surrounding soil during the cyclic phase. It can be seen, the ultimate post-cyclic pullout loads obtained from tests conducted in gravel 1 and gravel 2 were lower than the ultimate geocell loads obtained in tests with 10 cycles.

4. Conclusion

The present study evaluated the cyclic and post-cyclic pullout and interfacial behavior of geocells through a series of multi-stage pullout tests in sandy and gravelly soils. The effects of cyclic loading amplitude, number of cycles, load frequency, and cumulative displacement were investigated. However, some assumptions were performed and some other parameters such as the geocell type, relative density of soils, geocell height, cell aperture size, etc. could affect the obtained results which were considered as the study limitations in this evaluation. Hence, further studies are needed to investigate the effect of these parameters on the cyclic and post-cyclic pullout and interfacial behavior of geocells.

1. It was found that the ultimate post-cyclic pullout load of the geocell in sand, gravel 1 and gravel 2 was nearly 15%, 11% and 9% lower than the ultimate monotonic pullout load under the same vertical pressure, respectively. The increase in vertical pressure led to a decrease this difference and the ultimate pullout loads decreased 13%, 10%, and 5% for sand, gravel 1, and gravel 2, respectively. It was concluded that the reciprocating motion of loading during the cyclic phase partially broke the soil-to-geocell infill interlock. The pullout load then increased as the passive resistance in each geocell cellular was mobilized until all of the pullout capacity of the geocell had been contributed and the pullout load reached a steady state.
2. The loss of interaction during the cyclic phase lowered the ultimate pullout load in the post-cyclic phase in comparison with monotonic testing. The loss of strength of this interaction was dependent on the soil particle size. As it increased, the loss of interaction decreased from 15 % to 9% and 13% to 5% under 20 kPa and 60 kPa vertical pressure, respectively. Because the coarser soil formed a better interlock between the surrounding soil and geocell infill soil, which decreased the ability of the cyclic load to break each interlock. Moreover, the size of the soil particles affected the cumulative displacement during the cyclic phase, where the geocell displaced 4.7 mm in sandy soil which was decreased to 3.1 mm in gravel 2 under the same loading condition which showed geocell could be more freely displaced as the soil-to-soil interlock weakened or was broken.
3. Evaluation of the effect of loading amplitude and number of cycles indicated that an increase in the cyclic loading, number of cycles, and amplitude caused a decrease in the interaction between the geocell infill material and the surrounding soil resistance. Consequently, in gravel 1 and gravel 2 were 14% and 12.5% decreased in the ultimate post-cyclic pullout load than ultimate monotonic pullout load. As the interface stiffened with an increase in the vertical pressure and soil particle size, the reductive effect of loading amplitude decreased nearly 1.5%.
4. Contrary to the loading amplitude and number of cycles, the increase in frequency led to the development of the ultimate post-cyclic pullout load, which showed no significant

difference from the monotonic pullout behavior and multi-stage test results at 1 Hz. A comparison with previous research on planar geosynthetics showed that the effect of frequency could depend on the soil and geosynthetic complex properties and their response to the different frequency values. It was concluded that the increase in the load frequency led to compact the geocell infill materials. This compaction caused an increase in the ultimate post cyclic pullout load of the geocells.

References

[1] Basack, S., Karami, M., and Karakouzian, M. "Pile-soil interaction under cyclic lateral load in loose sand: Experimental and numerical evaluations", Soil Dyn. Earthquake Eng., **162**, pp. 1-10 (2022).

[2] El Sharnouby, M.M, and El Naggar, M.H. "Field investigation of lateral monotonic and cyclic performance of reinforced helical pulldown micropiles", Can. Geotech. J., **49**(5), pp. 560-573 (2018).

[3] Andavan, S. and Maneesh Kumar, B. "Case study on soil stabilization by using bitumen emulsions – A review", Mater. Today: Proceedings, **22**(3), pp. 1200-1202 (2020).

[4] Molaabasi, H., Semsani, S.N., Saberian, M., and et al. "Evaluation of the long term performance of stabilized sandy soil using binary mixtures: A micro and macro level approach", J. Cleaner Prod., **267**, pp. 1-18 (2020).

[5] Wu, S., Wei, Y., Zhang, Y., and et al. "Dynamic compaction of a thick soil stone fill: dynamic response and strengthening mechanics", Soil Dyn. Earthquake Eng., **129**, pp. 1-8 (2020)

[6] Latha, M. G., and Somwanshi, A. "Effect of reinforcement form on the bearing capacity of square footing on sand", Geotext. Geomembr., **27**(6), pp. 409-422 (2009).

[7] Yang, X., Han, J., Leshchinsky, D., and et al. "A three dimensional mechanistic empirical model for geocell reinforced unpaved roads", Acta Geotech., **8**, pp. 201-213 (2012).

[8] Tafreshi, S.N., Javadi, S., and Dawson, A.R. "Influence of geocell reinforcement on uplift response of belled piles", Acta Geotech., **9**, pp. 513-528 (2014).

[9] Mehdipour, I., Ghazavi, M., and Moayed, R.Z. “Stability analysis of geocell reinforced slopes using the limit equilibrium horizontal slice method”, Int. J. Geomech., **17**(9), pp. 1-15 (2017).

[10] Hegde, A. “Geocell reinforced foundation beds-past findings, present trends and future prospects: A state of the art review”, Constr. Build. Mater., **154**, pp. 658-674 (2017).

[11] Shiekh, I.R., and Shah, M.Y. “Experimental study on geocell reinforced base over dredged soil using static plate load”, Int. J. Pavement Res. Technol., **13**, pp. 286-295 (2020).

[12] Ardakani, A., and Namaei, A. “Numerical investigation on geocell reinforced slopes behavior by considering geocell geometry effect”, Geomech. Eng., **24**(6), pp. 589-597 (2021).

[13] Vieira, C.S., Ferreira, F.B., Pereira, P.M., and et al. “Pullout behavior of geosynthetics in a recycled construction and demolition material – effects of cyclic loading”, Transp. Geotech., **23**, pp. 1-17 (2020).

[14] Tafreshi, S.N., and Dawson, A.R. “A comparison of static and cyclic loading responses of foundations on geocell reinforced sand”, Geotext. Geomembr., **32**, pp. 55-68 (2012).

[15] Latha, M.G., and Manju, G.S. “Seismic response of geocell retaining walls through shaking table tests”, Int. J. Geosynth. Ground Eng., **2**, pp. 1-15 (2016).

[16] Biabani, M.M., Indraratna, B., and Ngo, N.T. “Modeling of geocell reinforced sub ballast subjected to cyclic loading”, Geotext. Geomembr., **44**(4), pp. 489-503 (2016).

[17] Pokharel, S.K., Han, J., Leshchinsky, D., and Parsons, R.L. “Experimental evaluation of geocell reinforced bases under repeated loading”, Int. J. Pavement Res. Technol., **11**(2), pp. 114-127 (2018).

[18] Xinye, H., Tomoharu, M., Toshihiko, K., and et al. “Seismic response of a newly developed geocell reinforced soil retaining wall backfilled with gravel by shaking table model test”, Geotechnical Hazards from large earthquakes and heavy rainfalls, pp. 513-523, Springer, Japan (2017).

[19] Venkateswarlu, H., Ujjawal, K.N., and Hegde, A. “Laboratory and numerical investigation of machine foundation reinforced with geogrids and geocell”, Geotext. Geomembr., **46**(6), pp. 882-896 (2018).

[20] Vnkateswarlu, H., Sharma, S., and Hegde, A. “Performance of genetic programming and multivariate adaptive regression spline models to predict vibration response of geocell reinforced soil bed: a comparative study”, Int. J. Geosynth. Ground Eng., **7**, pp. 1-17 (2021).

[21] Venkateswarlu, H., Raja, M.N.A., Hegde, A., and et al. “Experimental and intelligent modeling for predicting the amplitude of footing resting on geocell reinforced soil bed under vibratory load”, Transp. Geotech., **35**, pp. 1-14 (2022).

[22] Venkateswarlu, H., and Hegde, A. “Isolation prospects of geosynthetics reinforced soil beds subjected to vibration loading: experimental and analytical studies”, Geotech. Geol. Eng., **38**, pp. 6447-6465 (2020).

[23] Venkateswarlu, H., and Hegde, A. “Effect of influencing parameters on the vibration isolation efficiacy of geocell reinforced soil beds”, Int. J. Geosynth. Ground Eng., **6**, pp. 1-17 (2020).

[24] Venkateswarlu, H., and Hegde, A. “Behavior of geocell bed under vibration loading: 3D numerical studies”, Geosynth. Int., pp. 1-20 (2022), https://doi.org/10.1680/jgein.21.00050.

[25] Zhao, M.H., Zhang, L., Zou, X.J., and et al. “Research progress in two-direction composite foundation formed by geocell reinforced mattress and gravel piles”, China J. of Highway and Trans., **22**(1), pp. 1-10 (2009).

[26] Tavakoli, G.T.M, and Motarjemi, F. “Interfacial properties of geocell reinforced granular soils”, Geotext. Geomembr., **46**(4), pp. 384-395 (2018).

[27] Isik, A., and Gurbuz, A. “Pullout behavior of geocell reinforcement in cohesionless soils”, Geotext. Geomembr., **48**(1), pp. 71-81 (2020).

[28] Khedkar, M., and Mandal, J. “Pullout response of cellular reinforcement under low normal pressure”, Int. J. Geotech. Eng., **3**(1), pp. 75-87 (2013).

[29] Han, X., Kiyota, T., and Tatsuoka, F. “Interaction mechanism between geocell reinforcement and gravelly soil by pullout tests”, Bull. of Earth Resis. Struc., **46**, pp. 53-62 (2013).

[30] Fakharian, K., and Pilban, A. “Pullout tests on diagonally enhanced geocells embedded in sand to improve load-deformation response subjected to significant planar tensile loads”, Geotext. Geomembr., **49**(5), pp. 1229-1244 (2021).

[31] Guler, E., and Enunlu, A.K. “Investigation of dynamic behavior of geosynthetic reinforced soil retaining structures under earthquake loads”, Bull. Earthquake Eng., **7**, pp. 737-777 (2009).

[32] Fan, C., Liu, H., Cao, J., and et al. “Responses of reinforced soil retaining walls subjected to horizontal and vertical seismic loadings”, Soil Dyn. Earthquake Eng., **129**, pp. 1-10. (2020).

[33] Basbug, E., Cengiz, C., and Guler, E. “1-g Shaking table tests to determine the behavior of geosynthetic reinforced walls under seismic loads”, Transp. Geotech., **30**, pp. 1-12. (2021).

[34] ASTM D4253. “Standard test methods for maximum index density and unit weight of soils using a vibration table”, American Society for Testing and Materials (2016).

[35] ASTM D4254. “Standard test methods for minimum index density and unit weight of soil and calculation of relative density”, American Society for Testing and Materials (2006).

[36] ASTM D4595. “Standard method for tensile properties of geotextile by the wide-width strip method”, American Society for Testing and Materials (2023).

[37] Mahigir, A., Ardakani, A., and Hassanlourad, M. “Comparison between monotonic, cyclic and post cyclic pullout behavior of a PET geogrid embedded in clean sand and clayey sand”, Int. J. Geosynth. Ground Eng.. **7**, pp. 1-15 (2021).

[38] ASTM D6706. “Standard test method for measuring geosynthetic pullout resistance in soil”, American Society for Testing and Materials (2001).

[39] Moraci, N., and Cardile, G. “Influence of cyclic tensile loading on pullout resistance of geogrids embedded in a compacted granular soil”, Geotext. Geomembr., **27**, pp. 475-487 (2009).

[40] Zuo, Z., Yang, G., Wang, H., and et al. “Experimental investigation on pullout behavior of HDPE geogrid under static and dynamic loading”, Adv. Mater. Sci. Eng., **2020**, pp. 1-13 (2020).

List of Figures and Tables

Table 1. Soil properties

Properties	**Sand**	**Gravel 1**	**Gravel 2**
G_s	2.65	2.61	2.65
D_r (%)	70	70	70
Cu	1.88	1.7	1.99
Cc	0.94	1.15	1.24
γ_{dmax} (ton/m^3)	1.62	1.53	1.56
γ_{dmin} (ton/m^3)	1.37	1.43	1.4
γ_d (ton/m^3)	1.54	1.48	1.5
Φ (degree)	37.8	42.3	45.6
C (kPa)	4.13	1.03	0.98

Table 2. Geocell parameters

Property	Value
Cell area (cm × cm)	26.6 × 21.6
Geocell height (cm)	5
Geocell length (cm)	80
Geocell width (cm)	40
Ultimate longitudinal tensile strength (kN/m)	6.42
Ultimate transversal tensile strength (kN/m)	2.6
Seam peel strength at junctions (kN/m)	15
Elongation at break (%)	100

Table 3. The effect of 1 Hz frequency on the geocell behavior

Load amplitude (%)	20	30	40
Cumulative displacement (mm)	1.6	2	2.2
R value	0.005	0.01	0.015

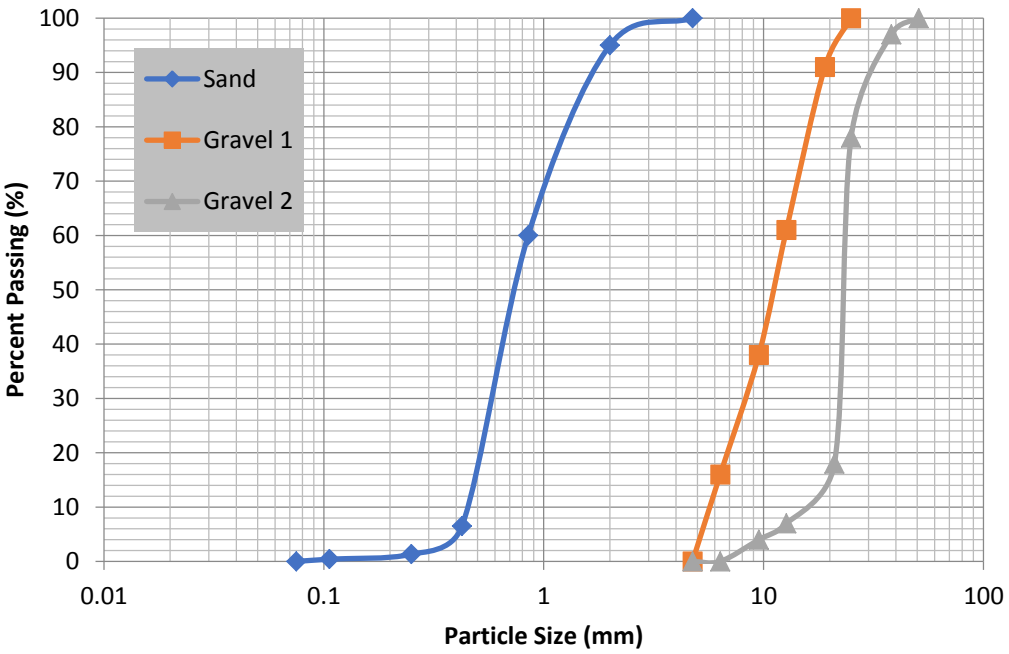

Fig. 1. Grain size distribution

Fig. 2. Image of apparatus

Fig. 3. Geocell placed on the lower half of soil sample

(a)

(b)

Fig. 4. Clamp designed for geocell-hydraulic jack attachment: (a) geocell attachment to clamp; (b) vertical plates

Fig. 5. Wire attachment to the geocell wall

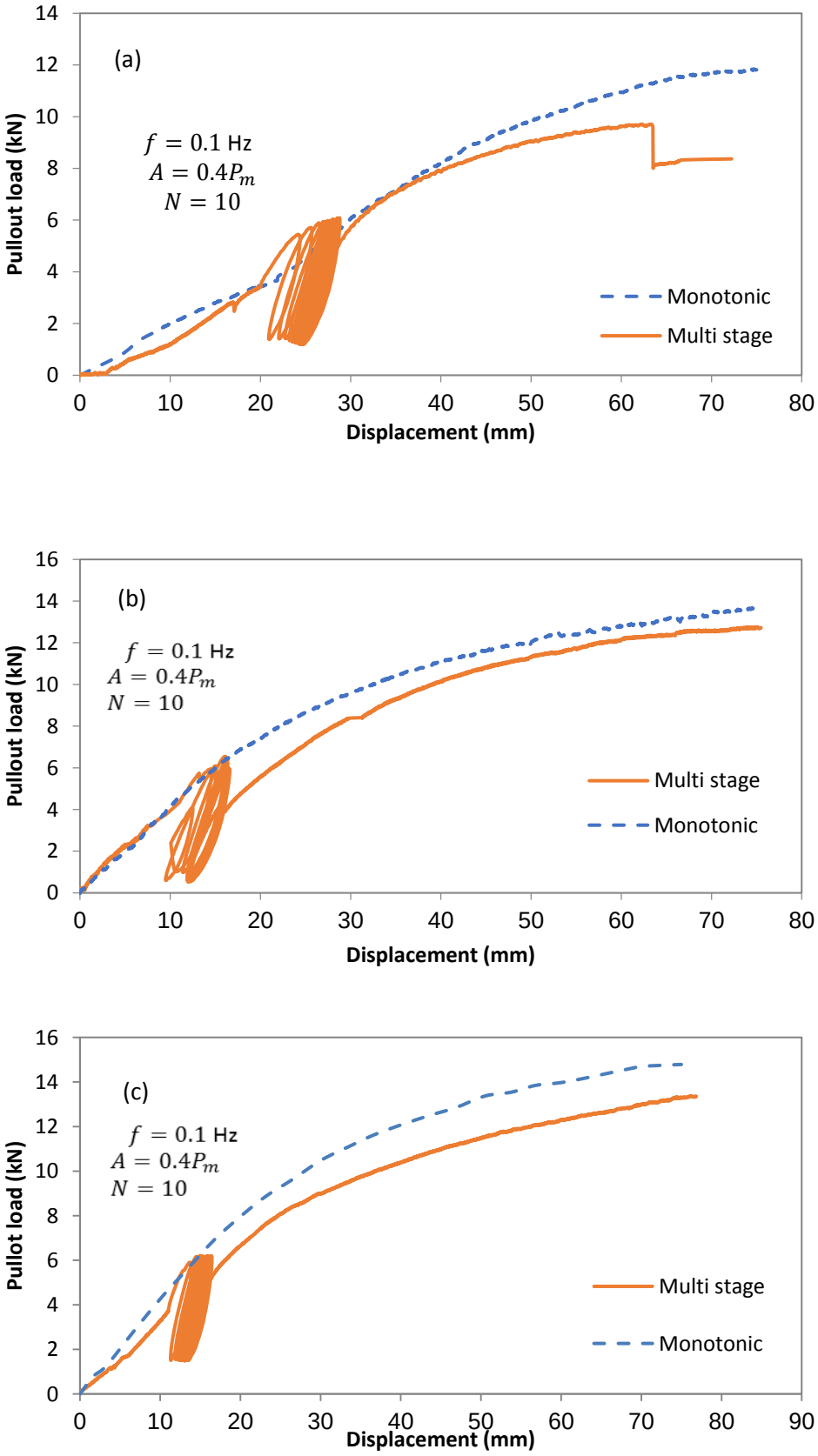

Fig. 6. Monotonic and multi-stage pullout test results under 20 kPa of vertical pressure: (a) sand; (b) gravel 1; (c) gravel 2

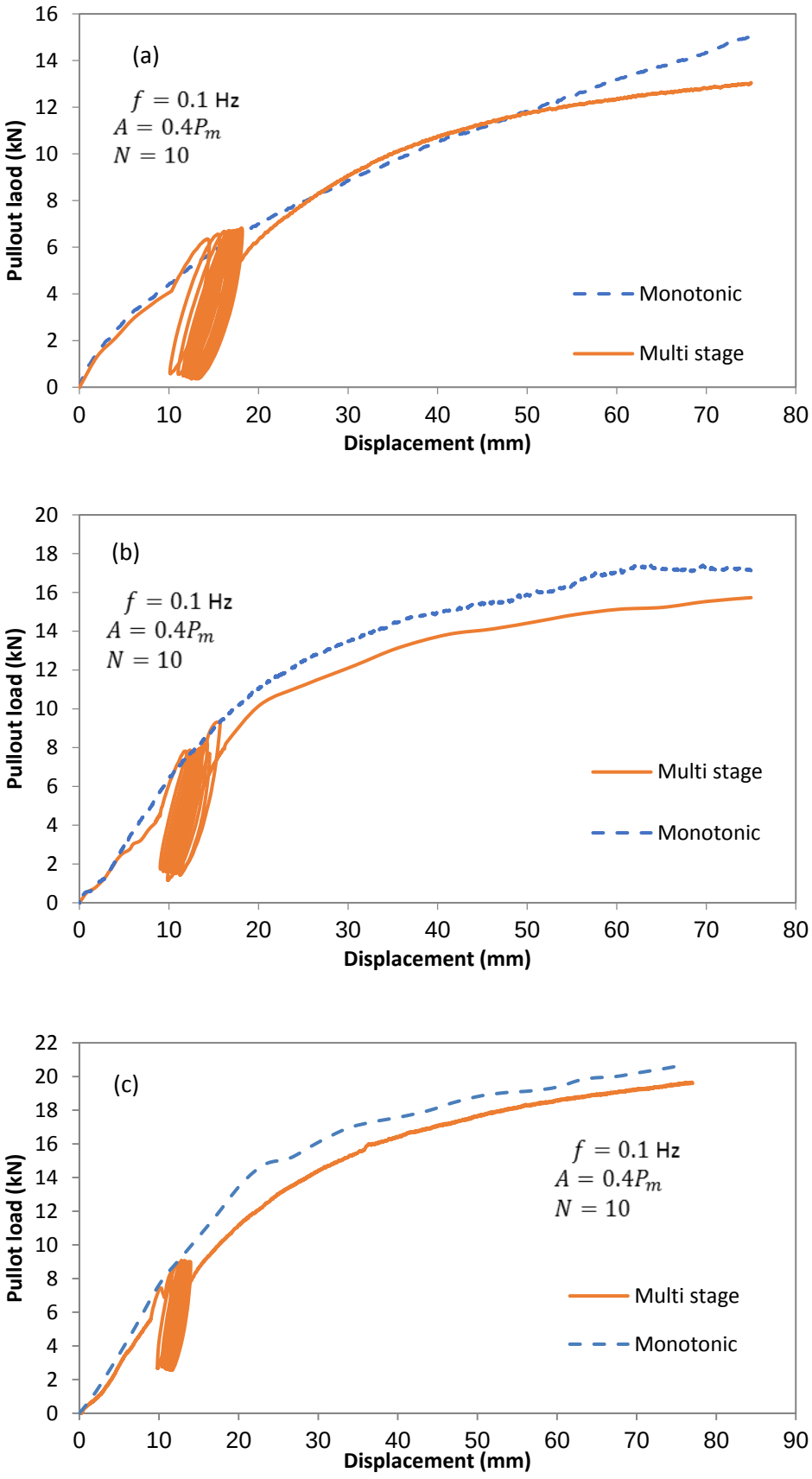

Fig. 7. Monotonic and multi-stage pullout test results under 60 kPa vertical pressure: (a) sand; (b) gravel 1; (c) gravel 2

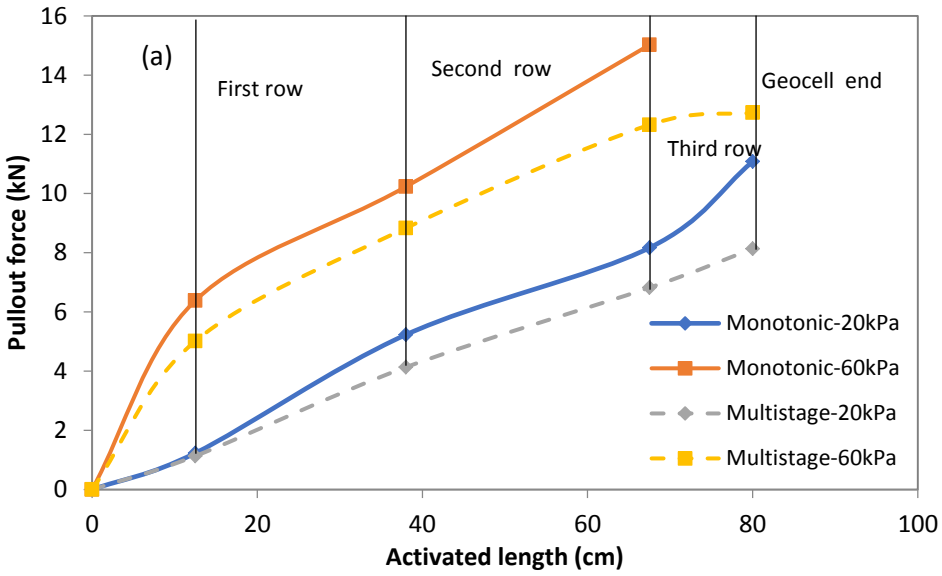
(a)
First row
Second row
Third row
Geocell end
Monotonic-20kPa
Monotonic-60kPa
Multistage-20kPa
Multistage-60kPa
Pullout force (kN)
Activated length (cm)
0
2
4
6
8
10
12
14
16
0
20
40
60
80
100

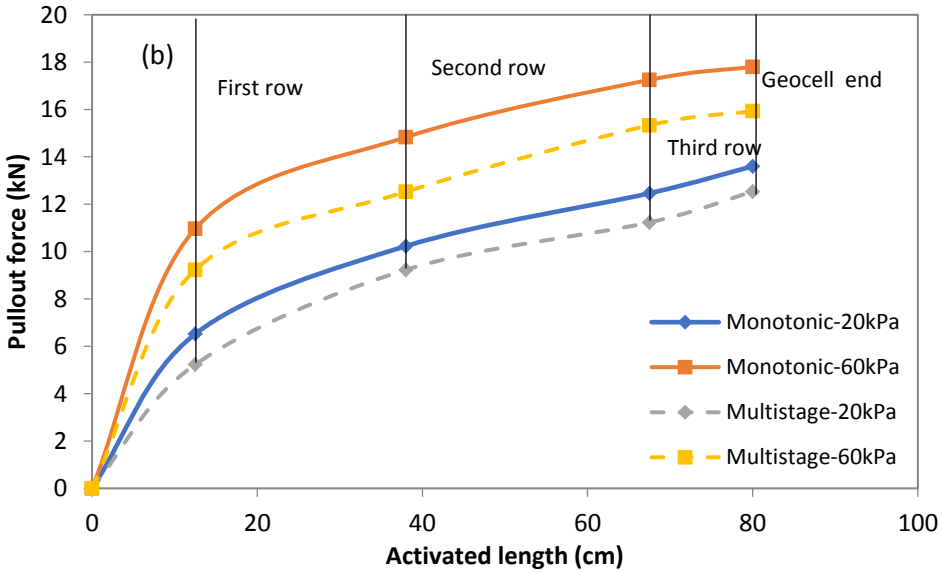
(b)
First row
Second row
Third row
Geocell end
Monotonic-20kPa
Monotonic-60kPa
Multistage-20kPa
Multistage-60kPa
Pullout force (kN)
Activated length (cm)
0
2
4
6
8
10
12
14
16
18
20
0
20
40
60
80
100

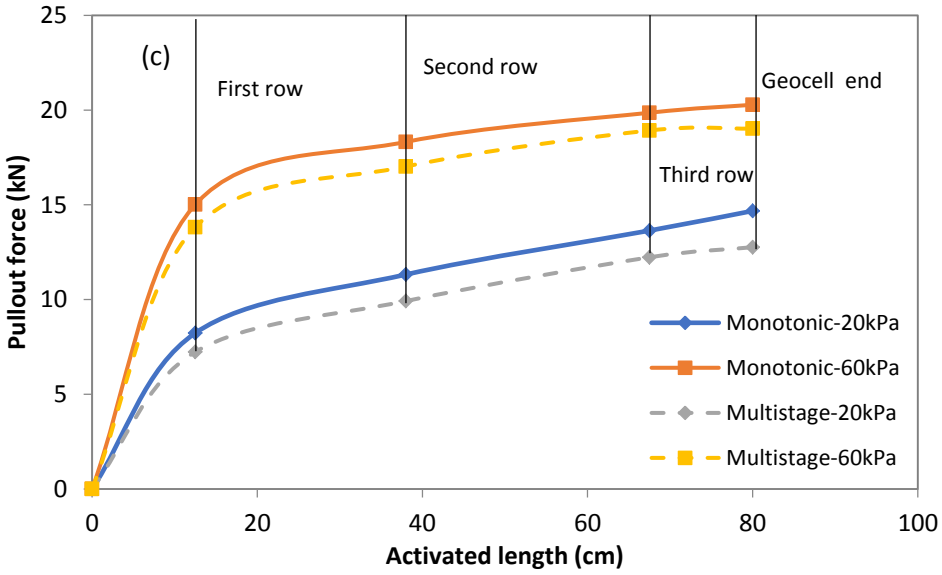

Fig. 8. Displacement distribution along geocell length: (a) sand; (b) gravel 1; (c) gravel 2

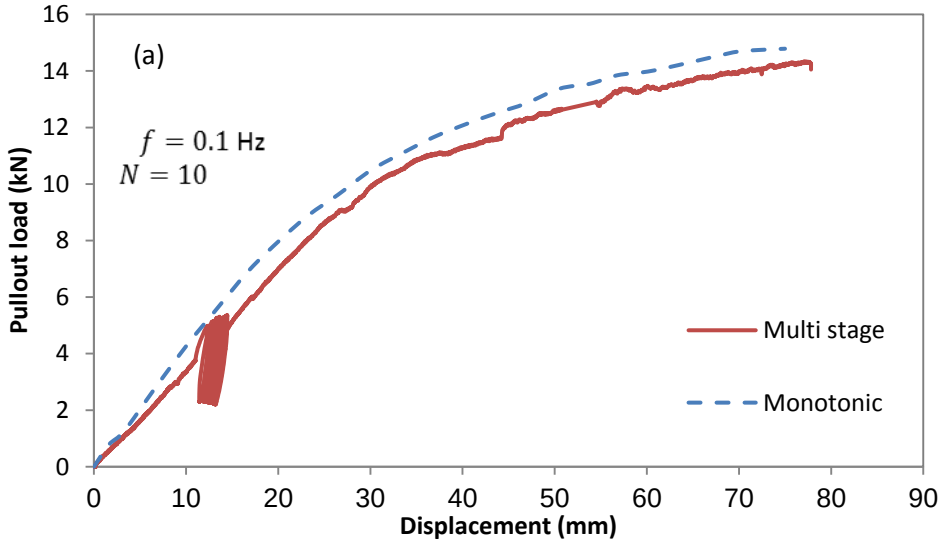

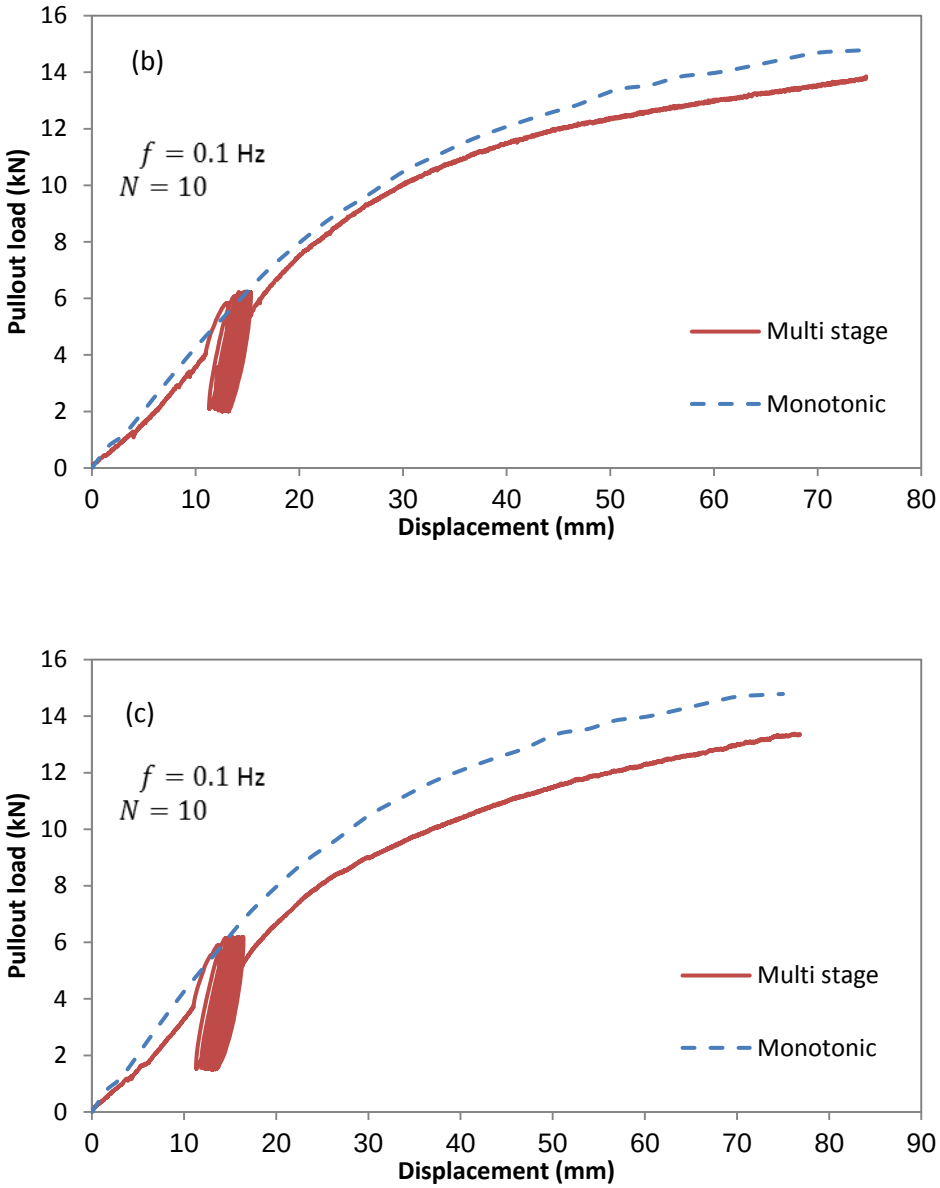

Fig. 9. Multi-stage pullout test at different cyclic load amplitudes under 20 kPa of vertical pressure: (a) 0.2 P_m; (b) 0.3 P_m; (c) 0.4 P_m

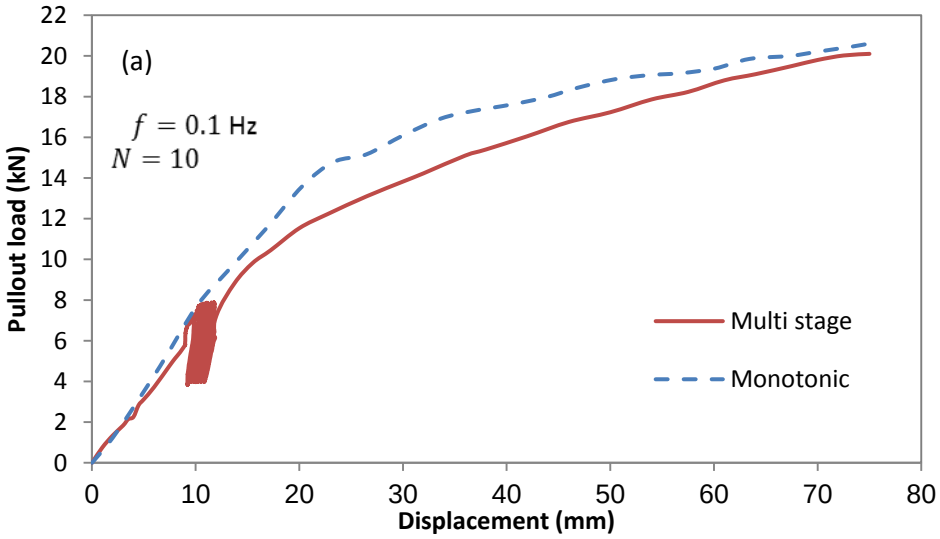
(a)
$f = 0.1$ Hz
$N = 10$
Pullout load (kN)
Displacement (mm)
Multi stage
Monotonic
0
2
4
6
8
10
12
14
16
18
20
22
0
10
20
30
40
50
60
70
80

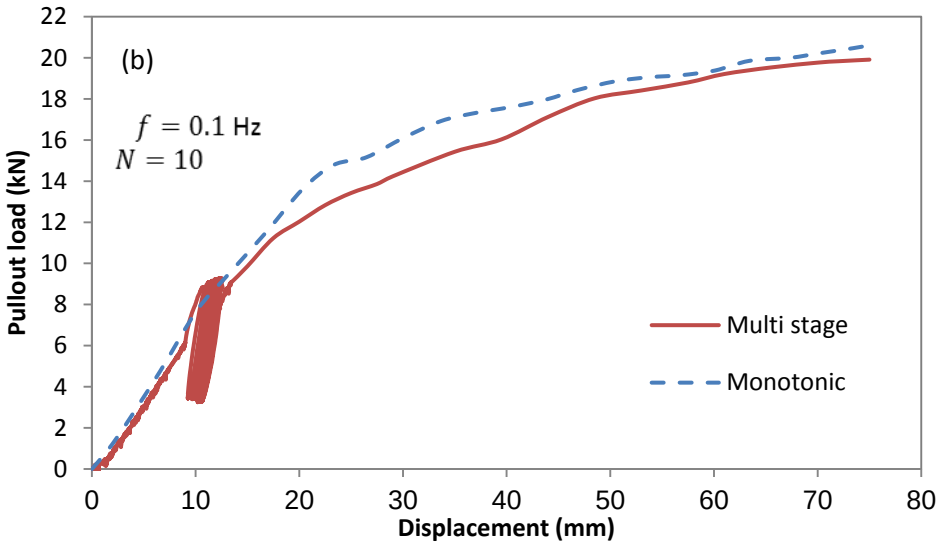
(b)
$f = 0.1$ Hz
$N = 10$
Pullout load (kN)
Displacement (mm)
Multi stage
Monotonic
0
2
4
6
8
10
12
14
16
18
20
22
0
10
20
30
40
50
60
70
80

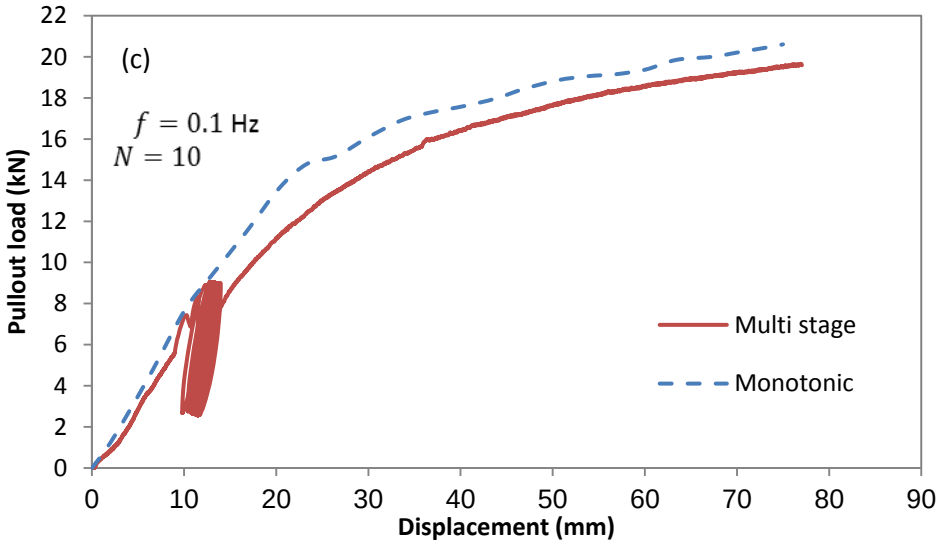

Fig. 10. Multi-stage pullout test at different cyclic load amplitudes under 60 kPa of vertical pressure: (a) 0.2 P_m; (b) 0.3 P_m; (c) 0.4 P_m.

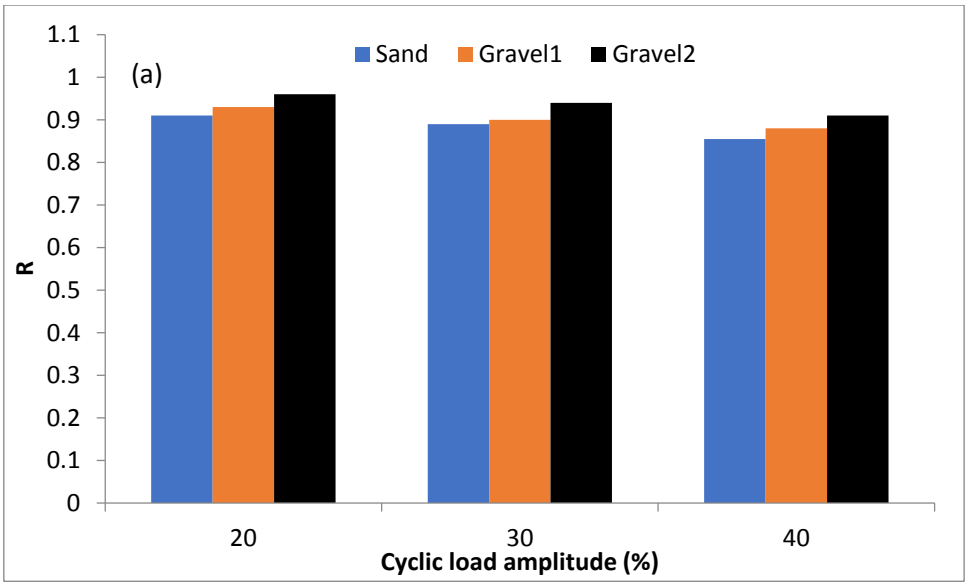

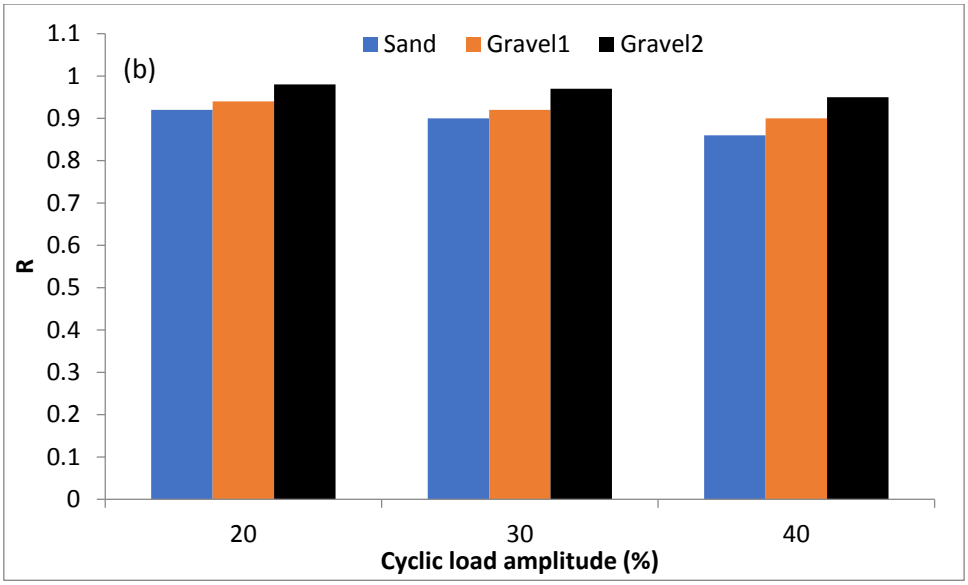

Fig. 11. Effect of soil particle size on cyclic load amplitude: (a) 20 kPa; (b) 60 kPa

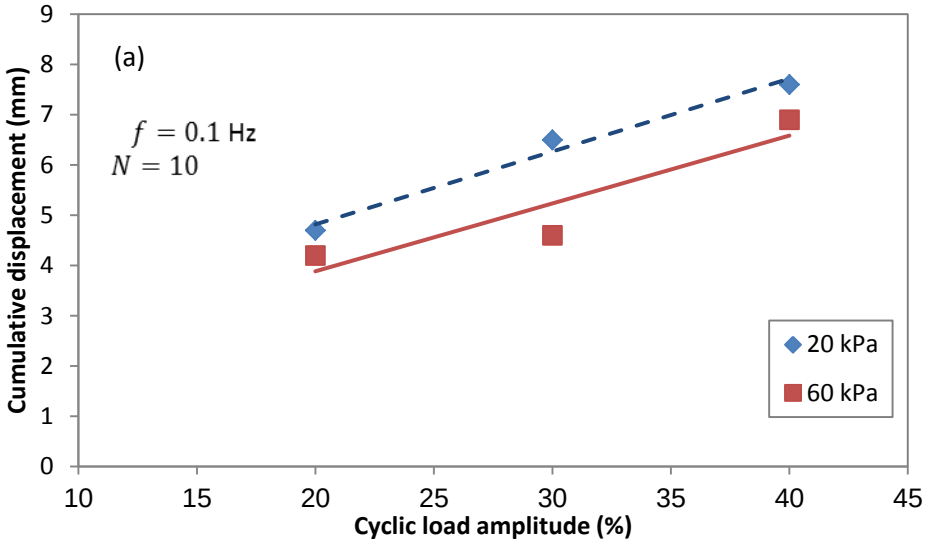
(a)
$f = 0.1$ Hz
$N = 10$
Cumulative displacement (mm)
Cyclic load amplitude (%)
20 kPa
60 kPa
0
1
2
3
4
5
6
7
8
9
10
15
20
25
30
35
40
45

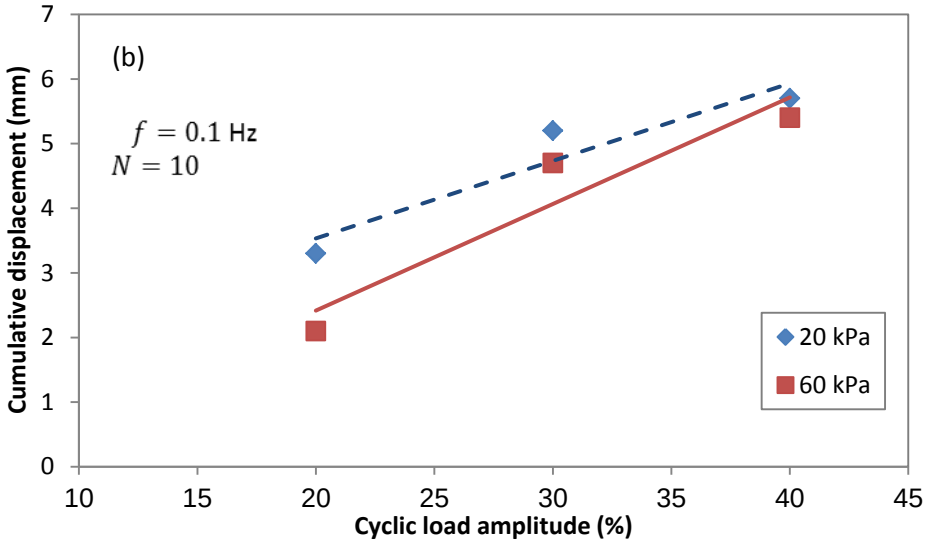
(b)
$f = 0.1$ Hz
$N = 10$
Cumulative displacement (mm)
Cyclic load amplitude (%)
20 kPa
60 kPa
0
1
2
3
4
5
6
7
10
15
20
25
30
35
40
45

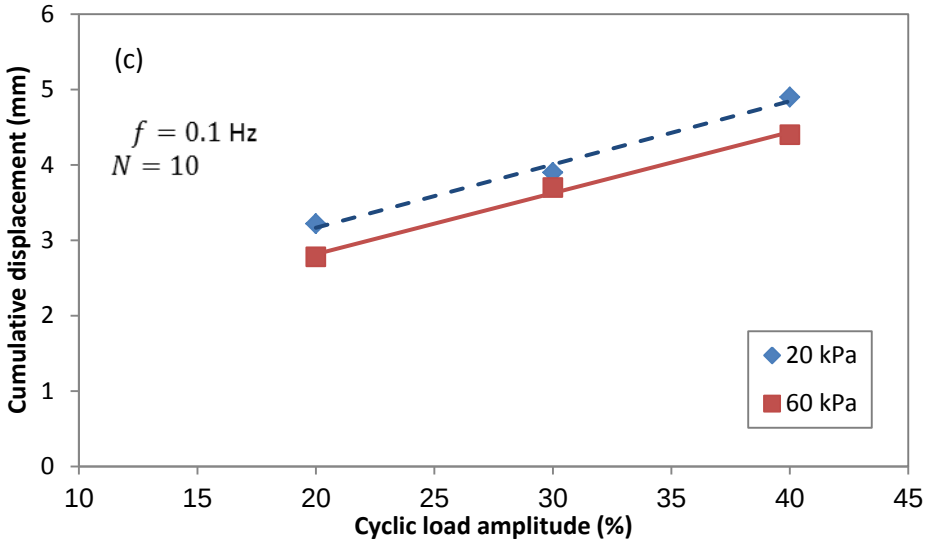

Fig. 12. Cumulative displacement induced during cyclic phase: (a) sand; (b) gravel 1; (c) gravel 2

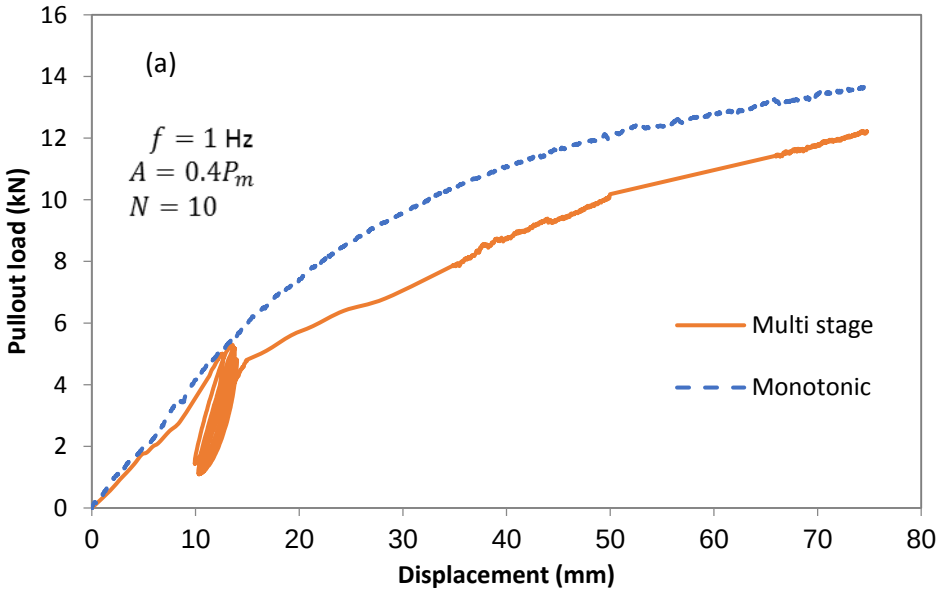

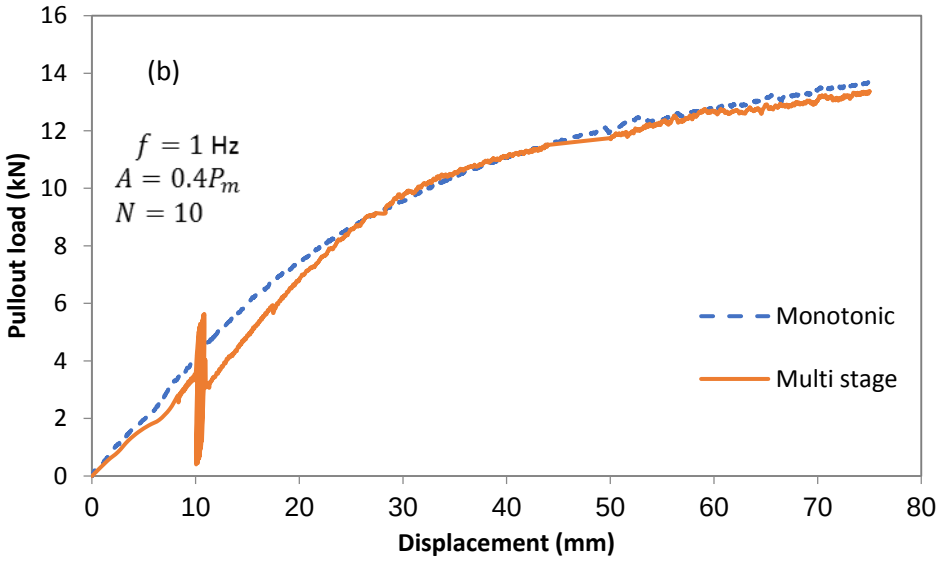

Fig. 13. Multi-stage load-displacement behavior of geocell in gravel 1: (a) 0.1 Hz; (b) 1 Hz

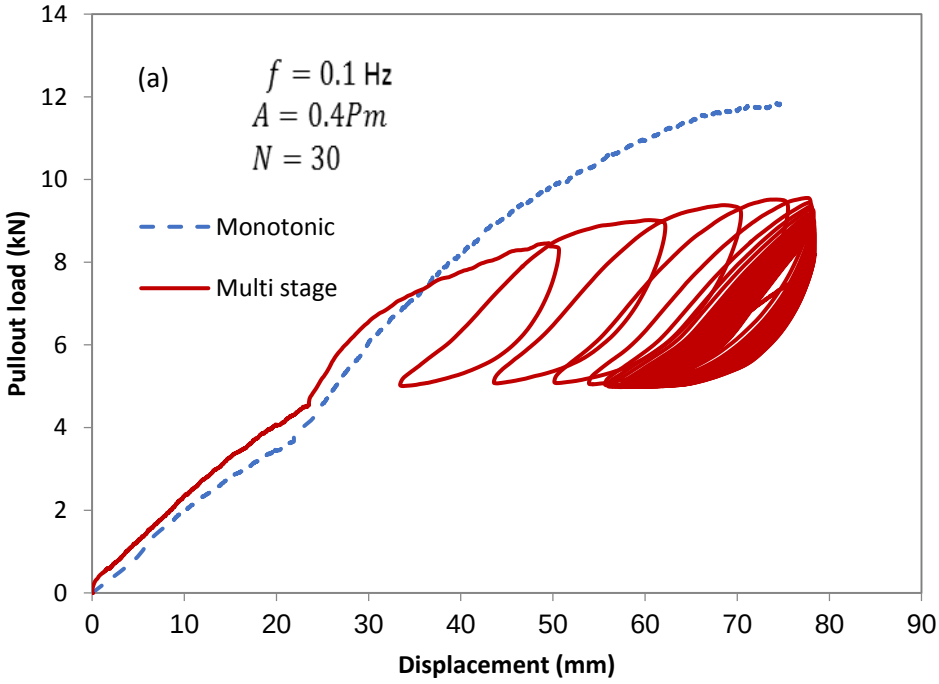

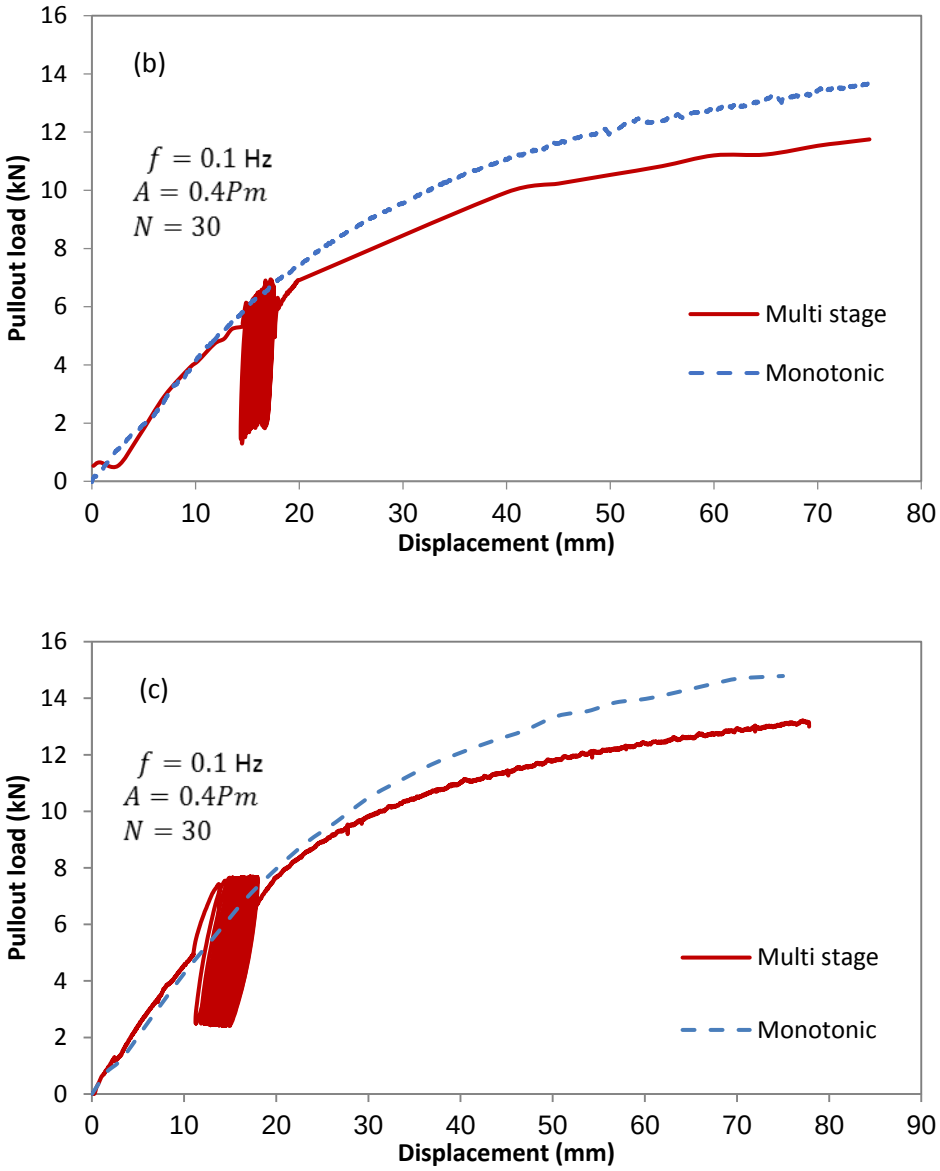

Fig. 14. Multi-stage test results for 30 cycles: (a) sand; (b) gravel 1; (c) gravel 2

Captions list

Table 1. Soil properties

Table 2. Geocell parameters

Table 3. The effect of 1 Hz frequency on the geocell behavior

Fig. 1. Grain size distribution

Fig. 2. Image and of apparatus

Fig. 3. Geocell placed on the lower half of soil sample

Authors Biography

Ali Namaei-kohal received the Ph.D. degree in geotechnical engineering from "Imam Khomeini international University" in 2022. Also, He received his M.S. degree from "Shahid Rajaee" University in 2017. His main research interests are application of geosynthetics and soil stabilization in geotechnical engineering.

Alireza Ardakani received the Ph.D. degree (with honors) in geotechnical engineering from “Tarbiat Modares” University in 2012. He is currently an associate professor in the department of civil engineering, Imam Khomeini International University, Qazvin. His main research interests are application of geosynthetics and waste material in geotechnical engineering.

Mahmoud Hassanlourad was born in Iran, 1977. He received the Ph.D. degree in geotechnical engineering from “Iran University of Science & Technology” in 2008. He is currently an associate professor in the department of civil engineering, Imam Khomeini International University, Qazvin.